Sensors and Actuators B 212 (2015) 78–83

Contents lists available at ScienceDirect

Sensors and Actuators B: Chemical

journal homepage: www.elsevier.com/locate/snb

Optical sensor for hydrogen gas based on a palladium-coated polymer microresonator

Mustafa Eryürek[a], Yasin Karadag[b], Nevin Taşaltın[c], Necmettin Kılınç[d], Alper Kiraz[a,e,*]

[a] Department of Physics, Koç University, Rumelifeneri Yolu, 34450 Sarıyer, İstanbul, Turkey
[b] Department of Physics, Marmara University, 34722 Göztepe, İstanbul, Turkey
[c] TUBITAK MRC Materials Institute, Sensor Materials-Photonic Technologies Lab., 41470 Gebze, Kocaeli, Turkey
[d] Mechatronics Engineering Department, Niğde University, 51245 Niğde, Turkey
[e] Koç University TÜPRAŞ Energy Center (KÜTEM), Koç University, Rumelifeneri Yolu, 34450 Sarıyer, İstanbul, Turkey

ARTICLE INFO

Article history:
Received 13 October 2014
Received in revised form 22 January 2015
Accepted 22 January 2015
Available online 7 February 2015

Keywords:
Hydrogen sensor
Whispering gallery mode
Microdisk
SU-8
Palladium

ABSTRACT

We report an integrated optical sensor of hydrogen (H_2) gas employing an SU-8 polymer microdisk resonator coated with a palladium (Pd) layer and coupled to a single-mode optical waveguide. The sensing mechanism relies on the expansion in the Pd lattice due to palladium hydride formation in the presence of H_2. Strain induced in the microresonator then causes a red shift of the spectral positions of the resonator whispering gallery modes (WGMs) which is monitored using a tunable laser coupled to the waveguide. H_2 concentrations below the flammable limit (4%) down to 0.3% could be detected in nitrogen atmosphere at room temperature. For H_2 concentrations between 0.3 and 1%, WGM spectral positions shifted linearly with H_2 concentration at a rate of 32 pm/% H_2. Average response time of the devices was measured to be 50 s for 1% H_2. The proposed device concept can also be used to detect different chemical gases by using appropriate sensing layers.

1. Introduction

Thanks to its high energy conversion efficiency, non-toxic side products, and sustainable nature, hydrogen (H_2) attracts a lot of attention as an energy source [1,2]. H_2 is also widely employed in clinical, industrial, and environmental reservation applications. Main difficulties in using H_2 stem from its low flammable limit (4%) and small molecular volume which bring challenges in H_2 storage and sensing. To date, H_2 sensors have been demonstrated using different measurement methods such as thermal [3], electrical [4], mechanical [5], acoustic [6] or optical [7]. Among these, optical sensing techniques are generally convenient for achieving reversible sensing with low cost and compact devices. The first optical H_2 sensor relied on the interferometric detection of the length of a palladium (Pd)-coated optical fiber [8]. This work was followed by other optical H_2 sensor demonstrations including those employing reflection spectroscopy [9], reflectivity [10] or surface plasmon resonance phenomenon [11].

In this paper, we report a novel optical sensor of H_2 gas that employs a polymer microdisk microresonator coated with a palladium (Pd) sensing layer and optically coupled to a single-mode polymer waveguide. Microdisk cavities host high quality optical resonances called whispering gallery modes (WGMs) whose spectral positions are very sensitive reporters of the microresonator size and refractive index [12]. Our sensor detects the H_2 gas via monitoring the spectral position of the WGMs that changes due to the strain induced in the microresonator as a result of expansion in the Pd sensing layer upon the formation of palladium hydride. To determine the WGM positions, we employ a tunable laser coupled into the polymer waveguide. We report H_2 detection below the flammable limit down to 0.3%, with a linear response of the sensor in the H_2 concentration range between 0.3 and 1% and a typical response time on the order of 1 min for 1% H_2.

Up to now, elastic nature of polymer microring or microdisk microresonators has been exploited in numerous demonstrations such as strain sensing [13], ultrasonic detection for photoacoustic microscopy [14], and opto-mechanically tunable lasing [15]. Despite these, H_2 gas sensing using a polymer microring or microdisk microresonator has not been demonstrated yet. Solid silicon-on-insulator (SOI) ring resonators have been previously used for H_2 gas sensing [16]. In these experiments, H_2 was detected by monitoring the spectral change in WGMs caused by the local

* Corresponding author at: Department of Physics, Koç University, Rumelifeneri Yolu, 34450 Sarıyer, İstanbul, Turkey. Tel.: +90 212 3381701; fax: +90 212 3381559.
E-mail address: akiraz@ku.edu.tr (A. Kiraz).

http://dx.doi.org/10.1016/j.snb.2015.01.097
0925-4005/

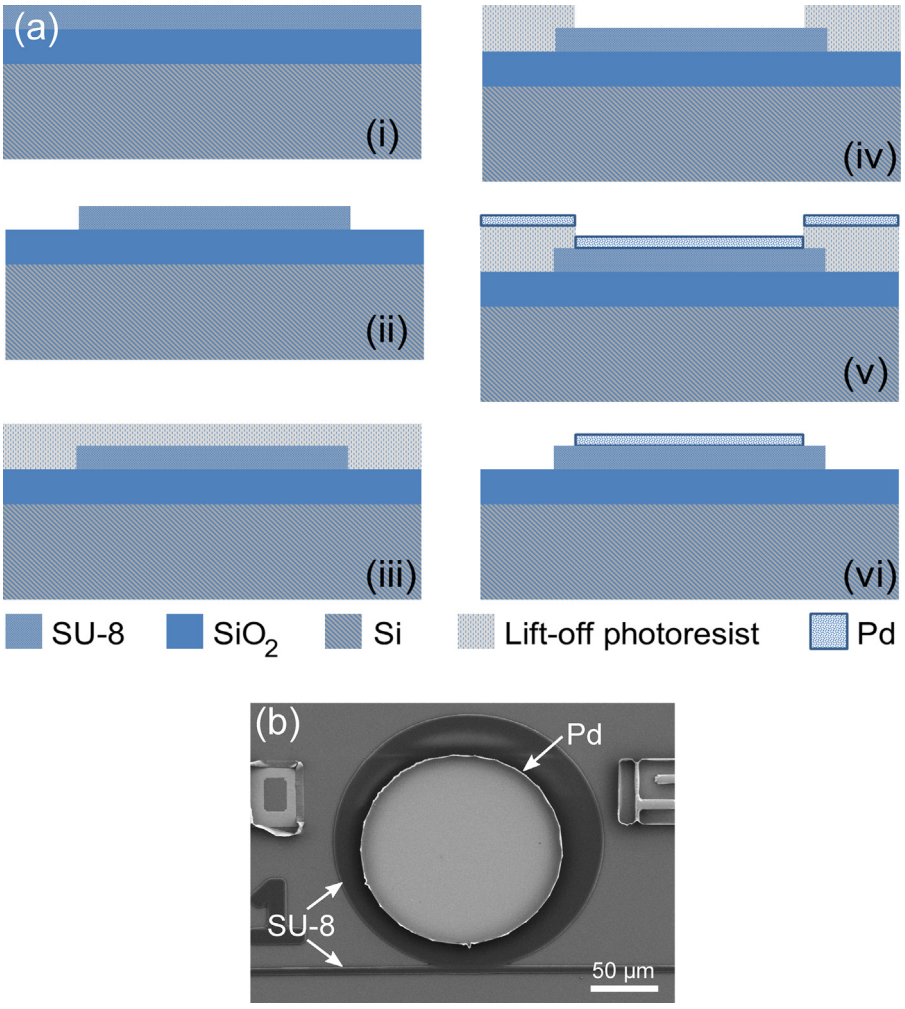

Fig. 1. (a) Cross-sectional schematic views showing the microfabrication steps of the sensor device. Thicknesses: Pd – 220 nm, SU-8 – 1200 nm, SiO_2 – 5 μm, Si – 500 μm. (b) SEM image of a 200-μm diameter Pd-coated SU-8 microresonator with SU-8 waveguide.

temperature increase resulting from the catalytic combustion of H_2. However, this approach did not allow measurement of H_2 concentrations lower than 0.7%. Vertical cavity lasers [17] were also used in microresonator-based H_2 gas sensing demonstrations. Here, H_2 gas sensing relied on the change of the complex refractive index of a Pd layer, leading to a spectral shift of the lasing wavelength. Compared to these previous demonstrations, our sensor combines easy fabrication together with the detection of relatively low H_2 concentrations (0.3%).

2. Experimental

2.1. Microfabrication

Two-step UV photolithography was used for the fabrication of the sensor devices (Fig. 1a). In the first step, SU-8 microresonators and waveguides were fabricated on a Si wafer with a 5 μm thick oxide layer using standard UV photolithography. The thicknesses of the microresonators and waveguides were measured as 1.2 μm. In the second step, a thin layer (thickness: 220 nm) of Pd was coated on the microresonators using RF plasma sputtering. Undesired portions of the Pd coating were removed using lift-off technique. The crystallographic properties of the Pd film were analyzed by X-ray diffraction (XRD) on a Rigaku Smarlab diffractometer (using Cu Kα = 1.5418 Å radiation) in the range of 10–90°. A Zeiss Ultra Plus field emission scanning electron microscope was used for SEM imaging.

Measurements reported in this paper employed disk-shaped microresonators with or without a hollow core as shown in Figs. 1b and 7. For the cases with a hollow core, the inner diameter was between 100 and 160 μm, substantially smaller than the 200 μm outer diameter of the microdisks. Hence, the optical properties of the WGMs were not affected by the presence of the hollow core. No considerable difference was observed between the sensing performance of the microdisk devices with or without a hollow core. For different microdisks, the diameter of the Pd-coated region was selected between 150 and 176 μm, smaller than the outer diameter (200 μm) to avoid absorption and scattering of WGMs due to the Pd layer (see Fig. 1b). We also made sure that the diameter of the Pd-coated region was larger than the inner diameter (100–160 μm) for the hollow core microdisks. Specific dimensions of the five sensors studied in this paper are: Sensor 1 – inner diameter = 160 μm, outer diameter = 200 μm, Pd-layer diameter = 176 μm; Sensor 2 – inner diameter = 100 μm, outer diameter = 200 μm, Pd-layer diameter = 150 μm; Sensor 3 – inner diameter = 0 μm, outer diameter = 200 μm, Pd-layer diameter = 176 μm; Sensor 4 – inner diameter = 160 μm, outer diameter = 200 μm, Pd-layer diameter = 176 μm; Sensor 5 – inner diameter = 100 μm, outer diameter = 200 μmi, Pd-layer diameter = 150 μm.

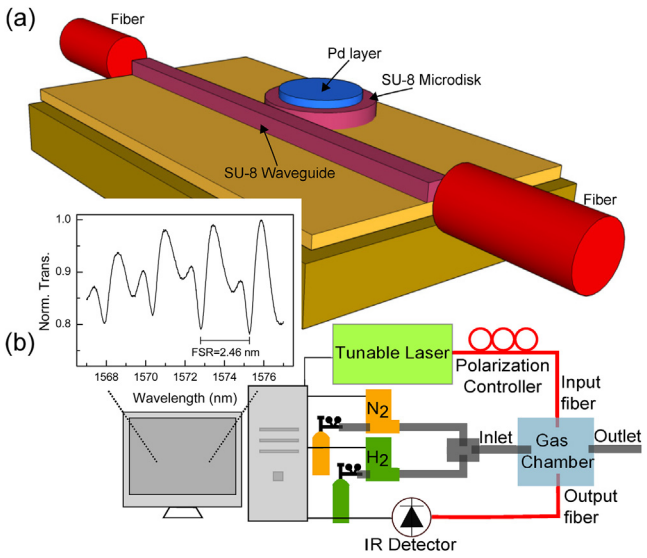

Fig. 2. Schematic description of (a) the sample and (b) the experimental setup. Inset shows a transmission spectrum obtained from a Pd-coated device.

2.2. Optical measurements

Optical measurements were performed using a tunable laser (Santec, TSL-510-C, tuning range: 1500–1630 nm, wavelength resolution: 1 pm) that was coupled from an optical fiber to individual waveguides using butt-coupling method [18] (see Fig. 2). Output light was collected using another optical fiber butt-coupled to the other end of the waveguide. Transmission spectra were obtained by recording the transmitted optical power using an InGaAs detector (Thorlabs, FGA10) and a current amplifier (Stanford Research Systems, SR570) while laser wavelength was swept over the wavelength range of interest. The sample was kept at room temperature (300 K) in a home-made gas chamber. Nitrogen (N_2) and H_2 gases were flown into the chamber using two mass flow controllers (Bronkhorst, EL-FLOW). During the experiments, the gas chamber was constantly purged with N_2 at a constant flow of 1000 mL/min while H_2 flow rate was adjusted for the desired H_2 concentration. In each experiment, before initiating the H_2 flow, N_2 was flown for at least 30 min in order to rule out the effects of humidity in the chamber. During this time, blue shift was observed in the spectral positions of the WGMs due to the decrease in relative humidity [19].

Inset in Fig. 2 shows an example of the transmission spectrum recorded from a Pd-coated microresonator. The quality factor (Q-factor) of the WGMs in this spectrum is determined to be around 1000 according to the formula $Q = \lambda/\delta\lambda$ where λ is the resonance wavelength and $\delta\lambda$ is the FWHM of the corresponding resonance mode. The dips in the spectrum correspond to the resonant wavelengths at which the light couples efficiently from the waveguide to the microresonator. For this device, the free spectral range (FSR) was measured to be 2.46 nm at around 1570 nm. This value is in a good agreement with the calculations using the effective index method that yield FSR = 2.50 nm, and with a result from the literature that employs a similar microdisk structure with 200 μm diameter where FSR = 2.28 nm was reported [20].

3. Results and discussion

Fig. 3 shows the XRD pattern of the Pd film. Two diffraction peaks are present at $2\theta = 40.1^\circ$ and 46.4° corresponding to [1 1 1] and [2 0 0] orientations of face-centered cubic (fcc) Pd, respectively.

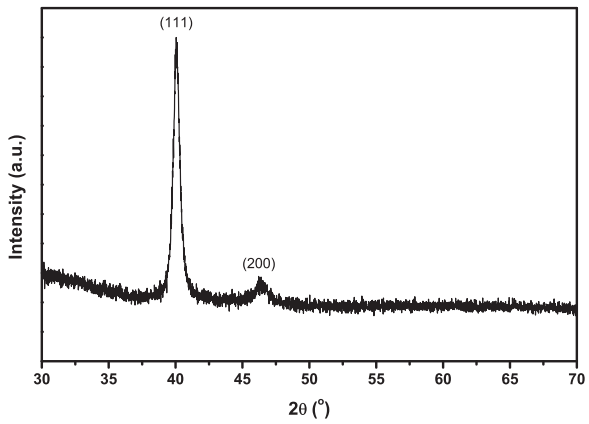

Fig. 3. XRD pattern observed from the 220 nm thick Pd film.

These peaks observed in the XRD pattern indicate a high purity and crystallinity in the Pd film. Similar XRD results have been observed for Pd thin films that prepared with different method such as electroplating, pulse laser deposition, laser ablation, and sputtering [21–24].

When they encounter the Pd surface, H_2 molecules disintegrate into hydrogen ions in the Pd lattice, forming palladium hydride, PdH_x, where x denotes the hydrogen ratio in the palladium hydride. Formation of PdH_x causes an increase in the lattice constant of Pd. Since SU-8 is an elastic polymer, this expansion of the Pd layer is transferred to the SU-8 microresonator as an increase in its diameter. Consequently, a red shift is observed in the resonance wavelengths of the WGMs because of the change in the radii of the SU-8 microresonators, as shown in Fig. 4. This constitutes the working principle of our sensor.

Fig. 5 shows spectral shifts ($\Delta\lambda$) observed for an uncoated SU-8 microdisk with 200 μm diameter (Fig. 5a) and Pd-coated Sensor 1 (Fig. 5b) as H_2 is introduced onto the devices under a constant N_2 flow of 1000 mL/min. Varying H_2 concentrations used in these experiments are also shown in each plot. $\Delta\lambda$ values were determined by tracking the center of a transmission dip between consecutive spectral acquisitions using the center of mass calculation algorithm. Such an algorithm is among the most primitive ones used for localization of single fluorophores in super-resolution microscopy [25]. In our experimental conditions signal to noise ratio of individual transmission dips as seen in Fig. 4 was larger than 100. This enabled localization of the center of a transmission dip with an accuracy better than $\sim\delta\lambda/100$ ($\delta\lambda$ denotes the FWHM of the transmission dip) [26]. In some cases, additional correction of $\Delta\lambda$ values was implemented, taking into account a constant linear spectral drift of the WGMs independent of the H_2 concentration. For the uncoated device, red spectral shift of about 14 pm is observed for 10% H_2 concentration, as seen in Fig. 5a. This corresponds to a very low H_2 detection that can be mainly attributed to the refractive index change in SU-8 as a result of H_2 adsorption [27]. Consistent with the strain caused by the expansion of the Pd layer, a red shift is observed in the WGMs. For the case of the Pd-coated device, 29 pm red spectral shift is observed for 1% H_2 concentration. Changes of the refractive indices of SU-8 and Pd are other potential sources for the observed red spectral shift. We conclude these contributions are negligible for two reasons: (i) control experiments shown in Fig. 5a reveal much smaller H_2 detection sensitivity due to the refractive index change of SU-8 and (ii) in our sensor devices Pd layer does not cover the region near the rim of the microdisk where WGMs are residing. We also note that a decrease in sensitivity of the devices was typically observed upon repeated cycles of H_2 exposure. This was attributed to the incomplete removal of hydrogen from the Pd lattice [28] and partial breaking of bonds between the Pd and

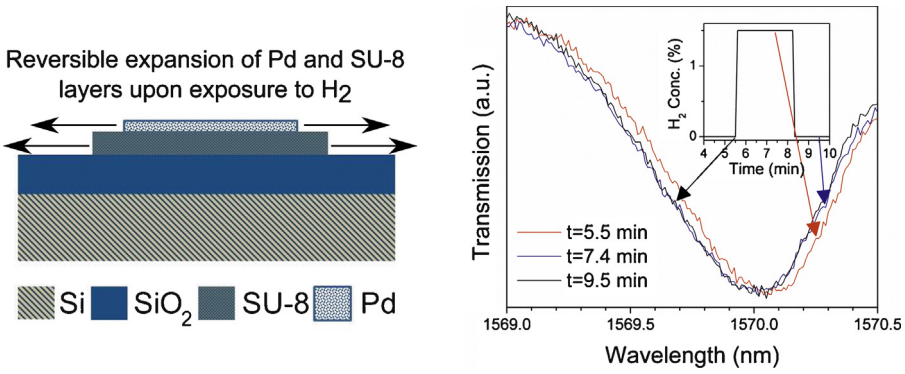

Fig. 4. Illustration of the H_2 sensing mechanism. Presence of H_2 leads to an expansion in the Pd layer. This results in a strain on the SU-8 microresonator that leads to a red shift of the WGMs. Graph shows reversible change in the spectral position of a WGM caused by exposure to 1.5% H_2.

SU-8 surfaces as discussed in the following paragraphs. For a given sensor device, we always used data recorded during the first set of experiments in calculating the sensitivity values reported in this paper.

Fig. 6a shows spectral shifts recorded from four different sensor devices for different H_2 concentrations. A linear trend is observed for concentrations up to 1% with a slope of 32 pm/% H_2. As compared to the uncoated device, this constitutes a 23-fold increase in H_2 detection sensitivity. Beyond 1% H_2 concentration, saturation is observed in the sensor response. This can be explained by the relatively small thickness of the Pd film and to the filling of the states available for hydrogen ions in the alpha-phase PdH_x [29].

It is known that for 1.5% H_2, Pd lattice constant undergoes 0.13% expansion [30]. For 1% H_2 and Pd layer radius of 75 μm, linear interpolation reveals the expansion of the radius of the Pd disk to be 65 nm. Assuming that the SU-8 microdisk expands by the same amount as the Pd layer and for SU-8 microdisk radius of 100 μm, the relation $\Delta r/r = \Delta\lambda/\lambda$ reveals an expected spectral shift of 1021 pm in the WGMs around 1570 nm for 1% H_2. The theoretical spectral shift predicted with this simple calculation is much larger than observed spectral shift of 32 pm for 1% H_2. We attribute this deviation to the different strengths of compressive and shear elastic forces applied from the Pd layer to SU-8 microdisk. As the SU-8 microdisk is attached to the underlying substrate over its whole cross-section, it will not fully follow the expansion in the Pd layer. A three dimensional computational analysis taking into account the substrate, and the thicknesses of Pd and SU-8 layers is necessary for accurate prediction of the H_2 sensitivity of our sensor devices. It is also likely that the shear forces between the expanding Pd layer and the SU-8 microdisk partially break the bonds between these two surfaces, leading to the observed irreversibility in the device operation. Expansion properties of the Pd layer are further investigated by the SEM images of a hollow core microdisk structure (inner and outer diameters of 110 and 200 μm) exposed to 20% H_2 for 30 min (Fig. 7). After exposure to H_2, considerable increase in the surface roughness of the Pd layer is observed in the regions where

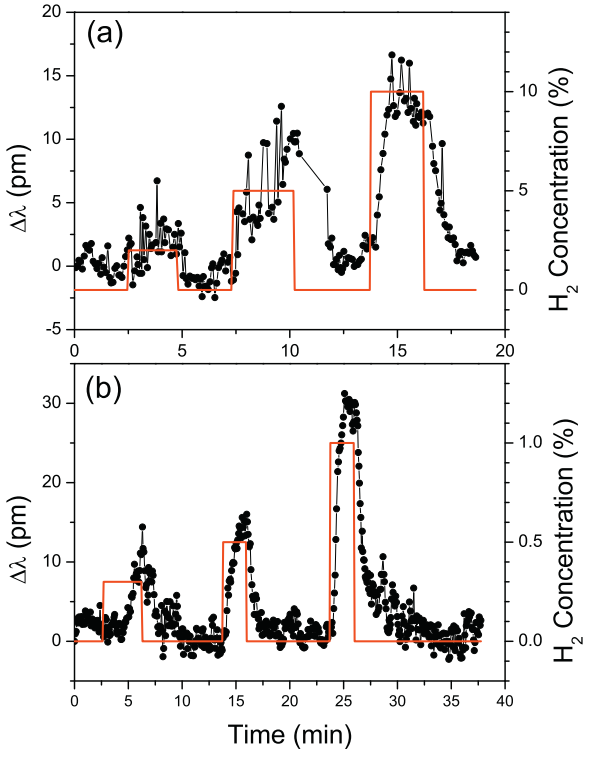

Fig. 5. Spectral shifts observed from (a) an uncoated and (b) a Pd-coated (Sensor 1) sensor device for different H_2 concentrations. Red lines show the dependence of H_2 concentration on time. (For interpretation of the references to color in this figure legend, the reader is referred to the web version of the article.)

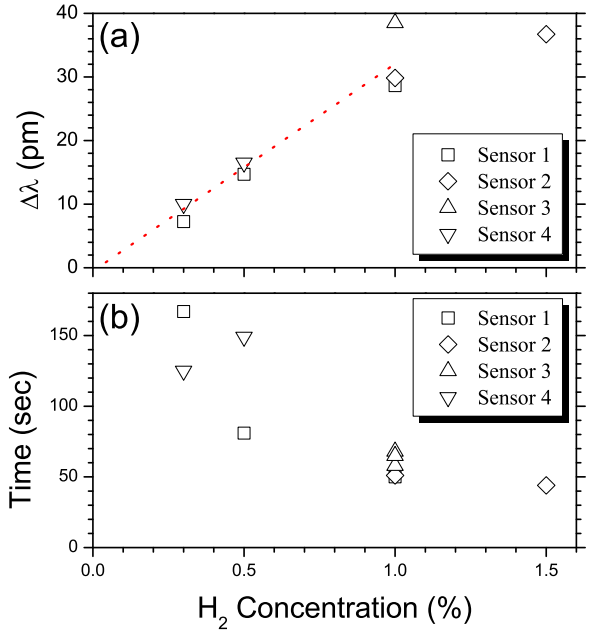

Fig. 6. (a) Spectral shifts measured from four different sensors at varying H_2 concentrations. Dashed red line is the best fit line for H_2 concentrations between 0.3 and 1%. (b) Response time measured for four different sensors at varying H_2 concentrations. (For interpretation of the references to color in this figure legend, the reader is referred to the web version of the article.)

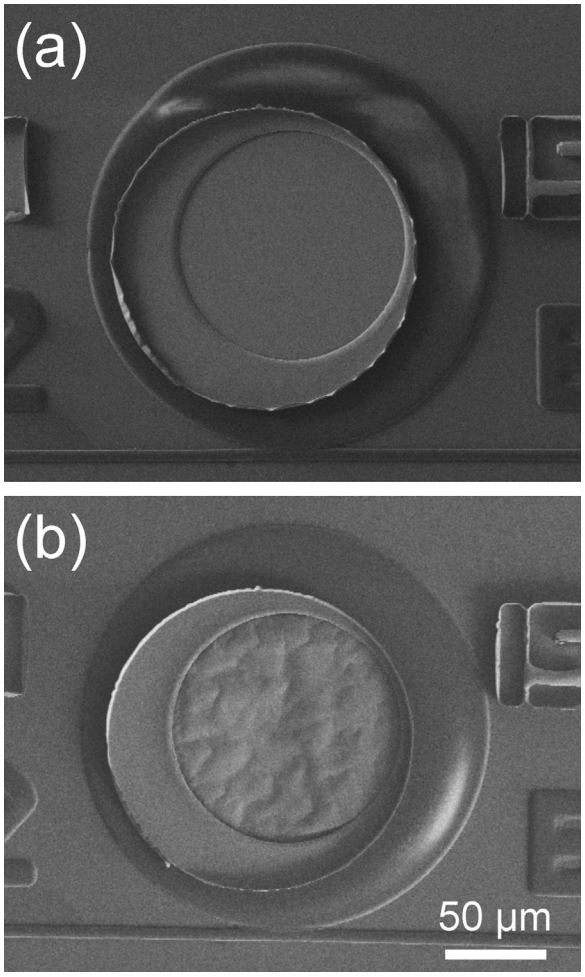

Fig. 7. SEM images of a Pd-coated SU-8 microring with inner and outer diameters of 110 and 200 μm before (a) and after (b) exposure to 20% H_2 for 30 min.

the Pd layer is in contact with SiO_2. Such a macroscopic degradation is not observed in the parts of the Pd layer that is in contact with the SU-8 surface. Despite this, we cannot rule out the presence of degradations at the interface between the Pd and SU-8 surfaces at the atomic scale. In the future, such degradation at the atomic scale can be avoided by using undercut regions between the SU-8 layer and substrate [31]. Such a geometry should better transmit the deformation of the Pd layer to the SU-8 microdisk, and thus enable better reversibility, better sensitivity and lower detection limits.

In our experiments, the lowest detected H_2 concentration was 0.3%. This value falls within the range of other optical H_2 sensors [16,17,32] and is well below the lower flammable limit of H_2 in air at room temperature (4%). The standard deviation in the spectral position of a resonance during stable experimental conditions is called wavelength stability of Pd coated SU-8 microdisk sensors. This value is determined to be lower than 2 pm under 1000 mL/min N_2 flow from the data presented in Fig. 5b between times t = 18 min and t = 23 min. This translates into a detection limit of 0.07% H_2 for our sensor devices for measurements in the concentration range between 0.3 and 1%. This limit can be further reduced by improving the quality factor (Q-factor) of the WGMs with higher resolution microfabrication. In addition, a better control can be implemented over the environmental conditions in the gas chamber. A parallel measurement scheme with a second uncoated SU-8 microdisk can also be employed in order to account for minute environmental fluctuations in the gas chamber.

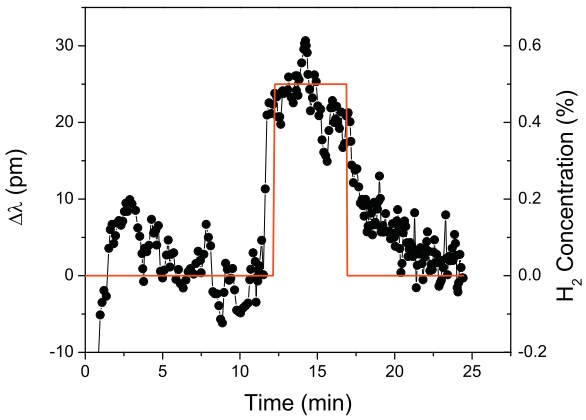

Fig. 8. Spectral shifts observed from a Pd-coated sensor device (Sensor 5) for different H_2 concentrations under 51% relative humidity. Red lines show the dependence of H_2 concentration on time. Spectral shifts and relative humidity were measured at room temperature (300 K). (For interpretation of the references to color in this figure legend, the reader is referred to the web version of the article.)

We observed that our sensor devices started to break down irreversibly as the H_2 concentration exceeded ~1.5%. This was due to the irreversible beta-phase formation in the PdH_x for $x > 1.5\%$ [30]. Hence the experimental dynamic range of our devices was 0.3–1.5% of H_2. This dynamic range can be increased by decreasing the lowest detection limit as discussed in the previous paragraph. In addition, the Pd sensing layer can also be replaced by other Pd alloys to further increase the beta-phase transition concentration [30]. It is well known for Pd expansion based hydrogen sensors that the ambient conditions (humidity and oxygen) deteriorate the sensor parameters such as sensitivity and response time. Such drawbacks that were previously reported for Pd coated micro/nano cantilever based hydrogen sensors [33,34] and Pd coated fiber Bragg grating sensors [35,36] should also be expected for the operation of the sensor device we demonstrate in this paper.

Preliminary experiments with our sensors under wet air conditions revealed a good sensing performance for 51% relative humidity (~20 pm spectral shift for 0.5% H_2) (Fig. 8), while almost no sensing performance could be observed for 100% relative humidity. A full understanding of our sensors under wet conditions requires detailed characterization of the performance of the uncoated and Pd-coated devices at different relative humidities.

For our sensor devices, response and recovery times were determined by analyzing the recorded time traces of the WGM spectral shifts shown in Fig. 5b. The response and recovery times correspond to the times required for the spectral shift to change by 90% of the total spectral change observed upon initiating or stopping the H_2 flow in the chamber, respectively. For the experimental data shown in Fig. 5b, the response and recovery times were calculated as 167, 81, 50 s and 55, 73, 163 s for 0.3, 0.5, and 1% H_2, respectively (see also Fig. 6b for the summary of the response dynamics of multiple devices). As expected, the response time decreases with increasing H_2 concentration. This behavior can be explained by the concentration-dependent surface adsorption of H_2 which represents the rate-limiting step in the PdH_x formation [37]. Similar trends were observed in the previously reported optical H_2 sensors [11,37]. The increase of the sensor recovery time with increasing H_2 concentration can be attributed to the delayed removal of hydrogen which has to undergo spatially constrained diffusion out of the Pd lattice.

4. Conclusions

In conclusion, using sensors based on optical signal readout, we have demonstrated detection of H_2 at room temperature with the

lower detection limit of 0.3% and the response time of 50 s for 1% H_2. Presented polymer microresonator sensors are low-cost, compact, and easy to fabricate. As compared to other state-of-the-art optical H_2 sensors, they hold a special promise for detecting extremely low H_2 concentrations. This can be achieved by increasing the *Q*-factors of the WGMs with higher resolution lithography techniques, having a better control over the environmental conditions in the gas sample chamber, and studying microdisks possessing undercut regions. With modified sensing coatings, this optical sensing platform is also suitable for detecting different gas species.

Acknowledgments

We acknowledge financial support from TÜBİTAK (grant no. 110T803). We thank Alexandr Jonáš for proofreading the manuscript and Suman Anand for fruitful discussions.

References

[1] C. Christofides, A. Mandelis, J. App. Phys. 68 (1990) R1.
[2] T. Hübert, L. Boon-Brett, G. Black, U. Banach, Sens. Actuators B 157 (2011) 329.
[3] E.-B. Lee, I.-S. Swang, J.-H. Cha, H.-J. Lee, W.-B. Lee, J.J. Pak, J.-H. Lee, B.-K. Ju, Sens. Actuators B 153 (2011) 392.
[4] F. Favier, E.C. Walter, M.P. Zach, T. Benter, R.M. Penner, Science 293 (2001) 2227.
[5] Y.-I. Chou, H.-C. Chiang, C.C. Wang, Sens. Actuators B 129 (2008) 72.
[6] S. Dong, F. Bai, J. Li, D. Viehland, Appl. Phys. Lett. 82 (2003) 4590.
[7] S.F. Silva, L. Coelho, O. Frazao, J.L. Santos, F.X. Malcata, IEEE Sens. J. 12 (2012) 93.
[8] M.A. Butler, Appl. Phys. Lett. 45 (1984) 1007.
[9] E. Maciak, Z. Opilski, Thin Solid Films 515 (2007) 8351.
[10] X. Bévenot, A. Trouillet, C. Veillas, H. Gagnaire, M. Clément, Sens. Actuators B 67 (2000) 57.
[11] X. Bévenot, A. Trouillet, C. Veillas, H. Gagnaire, M. Clément, Meas. Sci. Technol. 13 (2002) 118.
[12] A. Jonáš, Y. Karadag, M. Mestre, A. Kiraz, J. Opt. Soc. Am. B 29 (2012) 3240.
[13] B. Bhola, H.-C. Song, H. Tazawa, W.H. Steier, IEEE Photon. Technol. Lett. 17 (2005) 867.
[14] H. Li, B. Dong, Z. Zhang, H.F. Zhang, C. Sun, Sci. Rep. 4 (2014) 4496.
[15] A.M. Flatae, M. Buresi, H. Zeng, S. Nocentini, S. Wiegele, D. Wiersma, H. Kalt, CLEO, 2014.
[16] N.A. Yebo, D. Taillaert, J. Roels, D. Lahem, M. Debliquy, D.V. Thourhout, R. Baets, IEEE Photon. Technol. Lett. 21 (2009) 960.
[17] B.G. Griffin, A. Arbabi, A.M. Kasten, K.D. Choquette, L.L. Goddard, IEEE J. Quantum Electron. 48 (2012) 160.
[18] B. Bellini, A. dAlessandro, R. Beccherelli, Opt. Mater. 29 (2007) 1019.
[19] S. Schmid, S. Kühne, C. Hierold, J. Micromech. Microeng. 19 (2009) 1.
[20] S.-Y. Cho, N.M. Jokerst, IEEE Photon. Technol. Lett. 18 (2006) 2096.
[21] U. Singh, N. Jha, T.P. Singh, A. Kapoor, A. Perrone, Opt. Laser Technol. 42 (2010) 1128, ISSN 0030-3992.
[22] J. Keuler, L. Lorenzen, R. Sanderson, V. Prozesky, W. Przybylowicz, Thin Solid Films 347 (1999) 91, ISSN 0040-6090.
[23] C. Viespe, C. Grigoriu, Microelectron. Eng. 108 (2013) 218.
[24] A. Kobler, J. Lohmiller, J. Schaefer, M. Kerber, A. Castrup, A. Kashiwar, P.A. Gruber, K. Albe, H. Hahn, C. Kuebel, Beilstein J. Nanotechnol. 4 (2013) 554, ISSN 2190-4286.
[25] A. Small, S. Stahlheber, Nat. Methods 11 (2014) 267.
[26] T. Savin, P.S. Doyle, Biophys. J. 88 (2005) 623.
[27] S. Sato, T. Ose, S. Miyata, S. Kanehashi, H. Ito, S. Matsumoto, Y. Iwai, H. Matsumoto, K. Nagai, J. Appl. Polym. Sci. 121 (2011) 2794.
[28] J.I. Avila, R.J. Matelon, R. Trabol, M. Favre, D. Lederman, U.G. Volkmann, A.L. Cabrera, J. Appl. Phys. 107 (2010).
[29] D. Monzón-Hernández, D. Luna-Moreno, D. Martínez-Escobar, Sens. Actuators B 136 (2009) 562.
[30] J.-S. Noh, J.M. Lee, W. Lee, Sensors 11 (2011) 825.
[31] A. Flatae, T. Grossmann, T. Beck, S. Wiegele, H. Kalt, APL Mater. 2 (2014) 012107.
[32] M.Z. Alam, N. Carriere, F. Bahrami, M. Mojahedi, J.S. Aitchison, Opt. Lett. 38 (2013) 1428.
[33] D.R. Baselt, B. Fruhberger, E. Klaassen, S. Cemalovic, C.L. Britton Jr., S.V. Patel, T.E. Mlsna, D. McCorkle, B. Warmack, Sens. Actuators B: Chem. 88 (2003) 120 http://www.sciencedirect.com/science/article/pii/S0925400502003155, ISSN 0925-4005.
[34] J. Henriksson, L.G. Villanueva, J. Brugger, Nanoscale 4 (2012) 5059, http://dx.doi.org/10.1039/C2NR30639E.
[35] M. Yang, Z. Li, J. Dai, Z. Yang, Y. Zhang, Z. Zhuang, Meas. Sci. Technol. 24 (2013) 094009 http://stacks.iop.org/0957-0233/24/i=9/a=094009
[36] M. Yang, J. Dai, Photon. Sens. 4 (2014) 300, http://dx.doi.org/10.1007/s13320-014-0215-y, ISSN 1674-9251.
[37] Z. Zhao, Y. Sevryugina, M.A. Carpenter, D. Welch, H. Xia, Anal. Chem. 76 (2004) 6321.

Biographies

Mustafa Eryürek was born in Razgrad, Bulgaria in 1987. He received his B.Sc. degree from Bilkent University, Physics Department in 2010 and his M.Sc. degree from Koç University, Optoelectronics and Photonics Engineering Program in 2013. He is currently pursuing his Ph.D. in Koç University, Physics Department.

Yasin Karadag received his B.Sc. (2007) in physics from Bilkent University. He received his M.Sc. (2009) and Ph.D. degrees (2013) in physics from Koç University. In 2013, he joined TUBITAK BILGEM as a senior researcher where he worked on development of high power lasers. Since 2014, he has been an assistant professor at Marmara University, Physics Department.

Nevin Taşaltın received her B.Sc. (2002) and M.Sc. degrees (2005) in physics from Marmara University. She worked on development of various type gas sensors at TUBITAK Marmara Research Centre (MRC) as a researcher (2003–2006). She received Ph.D. degree (2010) in physics from Gebze Institute of Technology. Between 2010 and 2012 she worked at Koç University as a postdoctoral fellow. In 2012, she joined TUBITAK National Metrology Institute as a senior researcher where she worked on development of photonic devices. Since 2014, she has worked on development of nanostructures for photonic and sensor applications at TUBITAK MRC as an associate professor senior researcher.

Necmettin Kılınç received the B.Sc. degree from Marmara University, in 2003, and M.Sc. and Ph.D. degrees from Gebze Institute of Technology in 2006 and 2012, all in physics, respectively. After his Ph.D., he started to post doc at Optical Microsystems Laboratory, Koç University to research cantilever based biosensors. He is an assistant professor at Nigde University, Mechatronics Engineering Department, Nigde, Turkey. His research interests are fabrication of nanostructures and thin films of metal oxides and organic materials and structural and electrical properties of these materials and using these materials for bio-chemical sensor applications.

Alper Kiraz received his B.Sc. degree in electrical-electronics engineering from Bilkent University in 1998, M.Sc. and Ph.D. degrees in electrical and computer engineering from the University of California, Santa Barbara in 2000 and 2002, respectively. Between 2002 and 2004 he worked as a post-doctoral associate at the institute for physical chemistry in the Ludwig-Maximilians University, and received Alexander von Humboldt fellowship. He joined the Department of Physics of Koç University as an assistant professor in 2004. Currently, he is a professor in the same department. His research interests include optofluidics, single molecule spectroscopy/microscopy, and optical manipulation. Main applications targeted by his research are the development of novel biological and chemical sensors, optofluidic-based renewable energy solutions, and biomedical instruments. He is a member of OSA and SPIE.